Then Try This • Algorithmic Pattern Salon

Patterns in deep Mandelbrot zooms

Claude Heiland-Allen

Then Try This

Published on: Nov 11, 2023

URL: https://alpaca.pubpub.org/pub/uqh84mma

ABSTRACT

The Mandelbrot set emerges from iterations of $z \to z^2 + c$. Zooming deep into the fractal, history repeats each time the navigator veers off-centre, doubled up and twice as fast. At each resulting crisis, decisions allow patterns to be sculpted in the intricate shape of the boundary. Patterns in the decisions made when zooming are reflected in the complex dynamics, in particular in the binary expansions of the pairs of external rays landing on the cusp of each baby Mandelbrot set copy at the centre of each phase. Numerical and symbolic algorithms are used to analyze the pattern of decisions given the final coordinates of artworks by several fractal artists. New families of patterns can be synthesized, and from them coordinates can be calculated for image generation. In this way the manual labour of constructing deep Mandelbrot zooms can be reduced, allowing more time for pattern design.

Patterns in deep Mandelbrot zooms

The Mandelbrot set

The Mandelbrot set is a famous fractal (a complicated shape with detail visible at all scales) which emerges from the dynamics under iteration of the simple formula $z \to z^2 + c$.

The fractal contains a cardioid decorated with recursive trees of discs and thin filaments. Smaller copies of the whole ensemble appear in the filaments, interspersed with spirals with varying numbers of arms. Each solid region is associated with a positive whole number, called the period (there are multiple regions for each period in general). A child disk attached at internal angle $\frac{q}{p}$ has a period p times the period of its parent, and spirals in the filaments nearby have p arms (ordered by q in terms of size) [1].

For a gentle introduction to the Mandelbrot set see the first half of [2]. The radial edges in binary decomposition colouring are parts of external rays with terminating binary expansion. For a mathematical treatment of external rays, one of the key tools used to analyze locations, see [3].

Periodic (with repeating binary expansion) external rays land in pairs on the cusps of cardioids and bond points to disks (which have the same period as the rays) while pre-periodic (with eventually repeating binary expansion) external rays land on the centres of spirals [4]. Algorithms for converting between representations can be found in [5] [6].

Sources

The c-plane coordinates (centre and zoom factor) are essential for analyzing deep Mandelbrot zooms. Artists Jonathan Leavitt [7] [8], JWM [9] [10], FractalMonster [11], DinkydauSet [12], Microfractal [13], and Olbaid-ST [14], among others, have galleries of deep Mandelbrot set images with coordinates available.

It is unclear what license the coordinates are under, or even what kind of legal framework applies to coordinates. However, the artists JWM, DinkydauSet, and Microfractal have granted permission for images and analysis to be included in this paper. FractalMonster and Olbaid-ST also agreed but couldn't be included due to space constraints. No contact details for Jonathan Leavitt could be found.

Method

When constructing a deep Mandelbrot zoom image, there are generally relatively few decision points, because after each decision, the history repeats before anything new appears, increasing in speed and rotational symmetry by factors of two. If the artist decides not to change the focus of zooming, the repetition of history ends at a baby Mandelbrot set with rings of tiny details surrounding it.

Around half the way through the zoom is the last time a two-fold rotationally symmetric figure appears. This is typically when artists make decisions to vary the focus of the zoom, choosing a focus point not in the centre of the symmetry. Then zooming in to this new focus history repeats again, until the next decision point, which means the exponent in the magnification typically goes up by a factor of $\frac{3}{2}$ each time, for example from 10^{80} to 10^{120} to 10^{180}. Magnification depth is a limiting factor because deeper zooms require greater numerical precision which means images take longer to calculate.

By mathematically analyzing the behaviour of the coordinates under iteration, it is possible to deduce the decision points, and discover the patterns of nearby (pre)periodic points and their external rays.

There are several parts of the analysis. First is to find a sequence of increasing periods of nearby regions, at successive minima of $|z|$. Using Newton's root finding method, their locations can be found. Their distance from the coordinates of the original image gives the size of the view where a zooming decision was made. Images can then be generated to see what the decisions were.

More precisely, tracing external rays from near each region found determines their external angles. This is only feasible for low periods (below about 100000) as computation time increases rapidly. The periodic blocks of each angle pair can then be expressed as concatenations of the periodic blocks of lower period angle pairs in the sequence.

Analysis

0 and 1 are the binary digits that comprise external angles. The O and I columns contain P digits each. The corresponding external rays are these columns repeated with period P. O(p) and I(p) denote sequences of binary digits of length p, referring to earlier rows in the same table (different tables have different unrelated sequences). B^m denotes m copies of B concatenated together. n denotes the row of the table, so that O(P(n-1)) and I(P(n-1)) denote the sequences from the previous row of the table. X denotes a choice between O and I.

Choices may differ between the O and I columns, but the structure of the decomposition in terms of lower periods is the same. Choices are constrained by the row forming a ray pair.

“Polefcra” by Jonathan Leavitt

Figure 1
“Polefcra” by Jonathan Leavitt

Published 1998-2001, magnification 10^{100} [15].

Table 1

P (Period)	O(P) (Lower External Angle)	I(P) (Upper External Angle)
1	0	1
2	01	10
3	011	100

124	$O(3)^{25}$ 01 O(3) $I(3)^{14}$ 10	$O(3)^{25}$ 01 I(3) $O(3)^{14}$ 01
292	I(124) O(124) $I(3)^{14}$ 10	I(124) I(124) $O(3)^{14}$ 01
625	I(292) O(292) $I(3)^{13}$ 10	I(292) I(292) $O(3)^{13}$ 01
1294	I(625) O(625) $I(3)^{14}$ 10	I(625) I(625) $O(3)^{14}$ 01
2629	I(1294) O(1294) $I(3)^{13}$ 10	I(1294) I(1294) $O(3)^{13}$ 01

Pattern could be continued by repeating:

Table 2

P(n)	O(P(n))	I(P(n))
P(n-1) + P(n-1) + 44	I(P(n-1)) O(P(n-1)) $I(3)^{14}$ 10	I(P(n-1)) I(P(n-1)) $O(3)^{14}$ 01
P(n-1) + P(n-1) + 41	I(P(n-1)) O(P(n-1)) $I(3)^{13}$ 10	I(P(n-1)) I(P(n-1)) $O(3)^{13}$ 01

“Old Wood Dish” by JWM

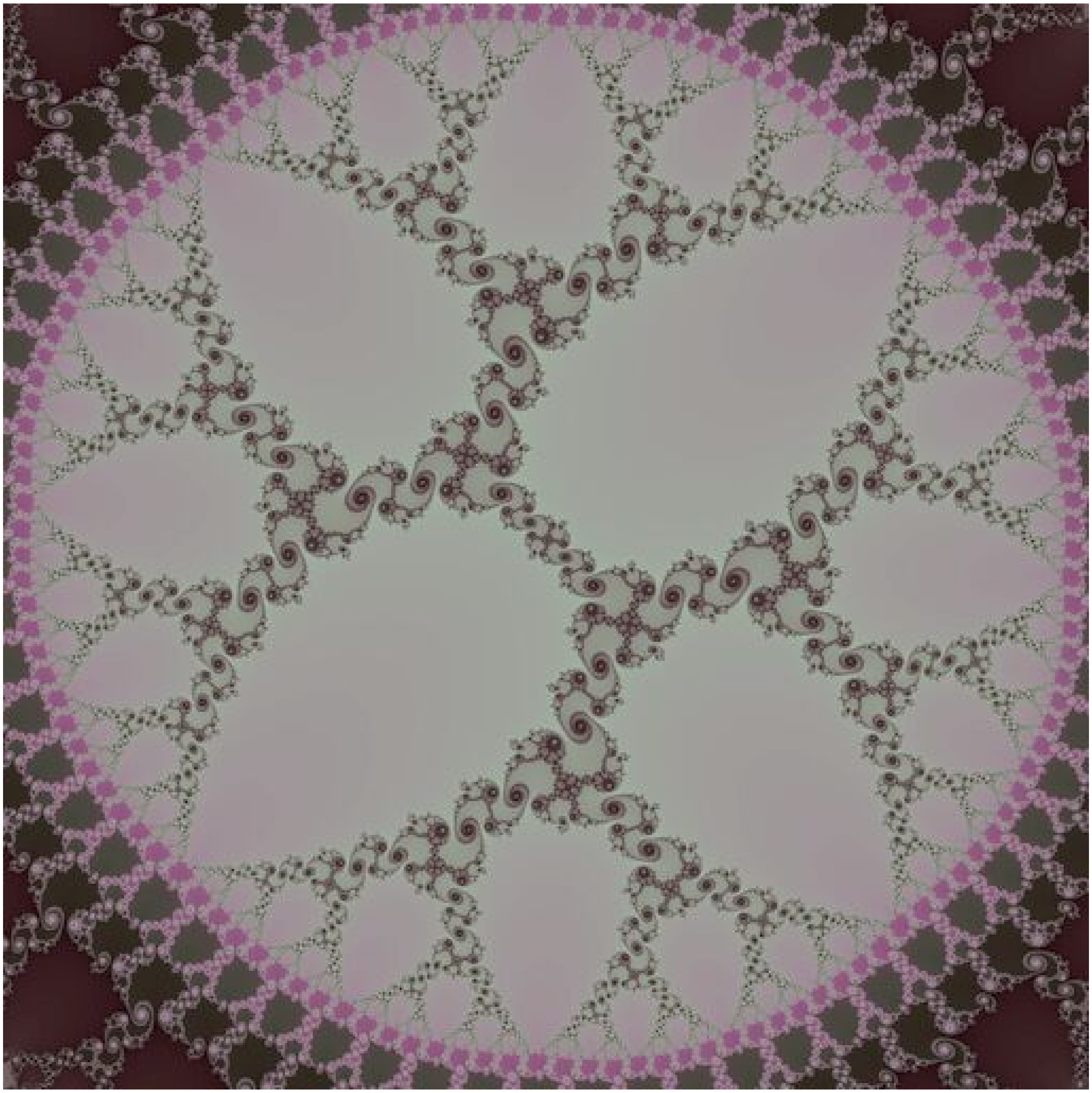

Figure 2
“Old Wood Dish” by JWM

Published 2010-11-25, magnification 10^{152} [16].

Table 3		
P (Period)	O(P) (Lower External Angle)	I(P) (Upper External Angle)
1	0	1

2	01	10
34	$O(2)^{15}$ 0111	$O(2)^{15}$ 1000
70	O(34) O(34) 11	O(34) I(34) 00
142	O(70) O(70) 11	O(70) I(70) 00
286	O(142) O(142) 11	O(142) I(142) 00
574	O(286) O(286) 11	O(286) I(286) 00
862	O(574) O(286) 11	O(574) I(286) 00
1438	I(862) O(574) 11	I(862) I(574) 00
2878	I(1438) O(1438) 11	I(1438) I(1438) 00
5758	O(2878) O(2878) 11	O(2878) I(2878) 00

The pattern is mostly a repetition of

Table 4

P(n)	O(P(n))	I(P(n))
P(n-1) + P(n-1) + 2	O(P(n-1)) O(P(n-1)) 11	O(P(n-1)) I(P(n-1)) 00

or its swapped (interchange O and I columns) and inverted (interchange 0 with 1 and O with I) version

Table 5

P(n)	O(P(n))	I(P(n))
P(n-1) + P(n-1) + 2	I(P(n-1)) O(P(n-1)) 11	I(P(n-1)) I(P(n-1)) 00

but at periods 862 and 1438 it deviates significantly.

“Evolution of Trees” by DinkydauSet

Figure 3
“Evolution of Trees” by DinkydauSet

Published 2013-09-25, magnification 10^{227} [17].

Table 6

P (Period)	O(P) (Lower External Angle)	I(P) (Upper External Angle)
1	0	1
93	$(10)^{45}$ 101	$(10)^{45}$ 110
145	I(93) $(10)^{25}$ 01	I(93) $(10)^{25}$ 10
3913	$(I(145)\ O(145))^{11}$ I(145) O(145) I(145) I(145) I(93) $(10)^{24}$ 10	$(I(145)\ O(145))^{11}$ I(145) I(145) O(145) O(145) I(93) $(10)^{24}$ 01
4348	I(3913) O(145) I(145) I(145)	I(3913) I(145) O(145) O(145)
8841	I(4348) O(4348) I(145)	I(4348) I(4348) O(145)

17628	O(8841) O(4348) I(4348) $(10)^{44}$ 101	O(8841) O(4348) I(4348) $(10)^{44}$ 110
35455	O(17628) I(8841) O(8841) I(145)	O(17628) I(8841) I(8841) O(145)
70910	I(35455) I(17628) O(8841) O(8841) I(145)	I(35455) I(17628) O(8841) I(8841) O(145)
141965	X(70910) X(35455) X(35455) X(145)	note 1
283930	X(141965) X(70910) X(70910) X(145)	note 1
567135	X(283930) X(141965) X(70910) X(35455) X(17628) X(8841) X(4348) X(3913) X(145)	note 2

1. Conjecture based on periods alone.
2. Conjecture based on periods alone. The step turns a tree into an S-shape.

The repeating part of the pattern seems to be

Table 7

P(n)	O(P(n)), I(P(n))
P(n-1)+P(n-2)+P(n-2)+145	X(P(n-1)) X(P(n-2)) X(P(n-2)) X(145)

“Mandelbrot Deep Julia Morphing 1” by Microfractal

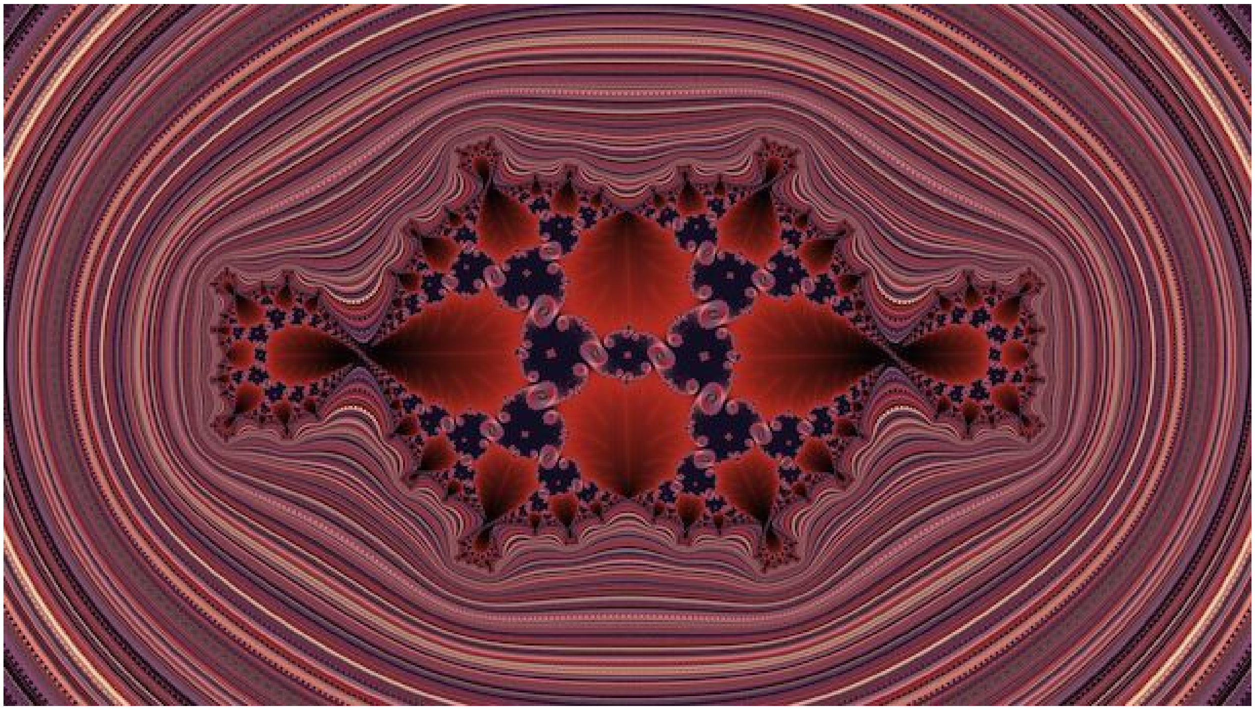

Figure 4
“Mandelbrot Deep Julia Morphing 1” by Microfractal

Published 2021-03-14, magnification 10^{4341} [18].

Table 8

P (Period)	O(P) (Lower External Angle)	I(P) (Upper External Angle)
1	0	1
2	01	10
3	011	100
4	0111	1000
8	O(4) I(4)	I(4) O(4)
137	$O(8)^{15}$ O(4) 1 O(8) I(4)	$O(8)^{15}$ O(4) 1 I(8) O(4)
278	I(137) O(137) I(4)	I(137) I(137) O(4)
560	I(278) O(278) I(4)	I(278) I(278) O(4)

1124	O(560) O(56O) I(4)	O(560) I(560) O(4)
2252	O(1124) O(1124) I(4)	O(1124) I(1124) O(4)
4508	I(2252) O(2252) I(4)	O(2252) I(2252) O(4)
9020	O(4508) O(4508) I(4)	O(4508) I(4508) O(4)
18044	I(9020) O(9020) I(4)	I(9020) I(9020) O(4)
36052	note 1	note 2
72144	X(36052) X(18044) X(18044) X(4)	note 3
144248	X(72144) X(36052) X(36052)	
288540	X(144248) X(72144) X(72144) X(4)	
577036	X(288540) X(144248) X(144248)	
1154120	X(577036) X(288540) X(288540) X(4)	
2308192	X(1154120) X(577036) X(577036)	
4616436	X(2308192) X(1154120) X(1154120) X(4)	

1. O(36052) = I(18044) I(9020) O(4508) I(2252) O(1124) O(560) I(278) O(137) O(8)^{15} I(4) 0 I(4)
2. I(36052) = I(18044) I(9020) O(4508) I(2252) O(1124) O(560) I(278) I(137) O(8)^{15} I(4) 1 O(4)
3. Conjectures based on periods alone.

The first pattern building a tree is similar to “Old Wood Dish” by JWM:

Table 9

P(n)	O(P(n))	I(P(n))
P(n-1)+P(n-1)+4	O(P(n-1)) O(P(n-1)) I(4)	O(P(n-1)) I(P(n-1)) O(4)

At period 36052 the tree is turned into an S. The second pattern is similar to “Evolution Of Trees” by DinkydauSet:

Table 10

P(n)	Notes
P(n-1)+P(n-2)+P(n-2)+4	Building a tree.
P(n-1)+P(n-2)+P(n-2)	Making an S.

Synthesis

“Polefcra” variations

Table 11

P(n) (Period)	O(P) (Lower External Angle)	I(P) (Upper External Angle)
1	0	1
2	01	10
3	011	100
P(n-1) + 1	O(P(n-1)) 1	I(P(n-1)) 0
m	011…11	100…00
40 × m + 4	$O(m)^{26}$ 01 O(m) $I(m)^{13}$ 10	$O(m)^{26}$ 01 I(m) $O(m)^{13}$ 01
2 × P(n-1) + 14 × m + 2	I(P(n-1)) O(P(n-1)) $I(m)^{14}$ 10	I(P(n-1)) I(P(n-1)) $O(m)^{14}$ 01
2 × P(n-1) + 13 × m + 2	I(P(n-1)) O(P(n-1)) $I(m)^{13}$ 10	I(P(n-1)) I(P(n-1)) $O(m)^{13}$ 01

Repeating the two last lines k times increases the number of rings of reverse bifurcation. Increasing m increases the spacing between the rings of reverse bifurcation. The original “Polefcra” by Jonathan Leavitt corresponds to k = 4 and m = 3. Images drawn with k = 4 and m = 3 except for the variable under consideration.

Table 12

	1	2	3	4	5	6

k	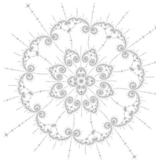 Figure 5	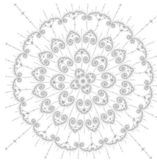 Figure 6	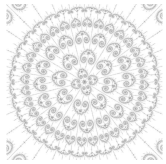 Figure 7	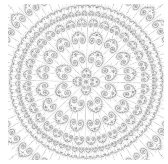 Figure 8	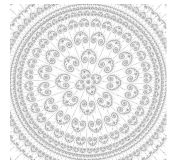 Figure 9	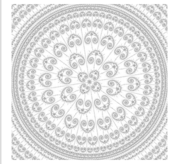 Figure 10
m-2	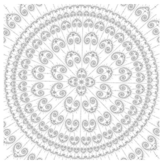 Figure 11	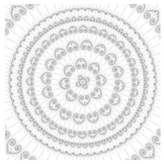 Figure 12	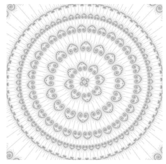 Figure 13	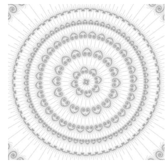 Figure 14	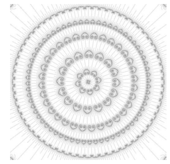 Figure 15	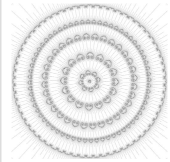 Figure 16

“Old Wood Dish” variations

Table 13

P(n) (Period)	O(P) (Lower External Angle)	I(P) (Upper External Angle)
1	0	1
2	01	10
k × 2 + 2 + m	$O(2)^k$ O(2) 1^m	$O(2)^k$ I(2) 0^m
2 × P(n-1) + m	O(P(n-1)) O(P(n-1)) 1^m	O(P(n-1)) I(P(n-1)) 0^m

where the last line is repeated to refine the structure. Increasing m lengthens the branches of the tree: Increasing k tightens the spirals the tree is made of: The original “Old Wood Dish” by JWM corresponds to m = 2, k = 15. Images drawn with m = 2, k = 15 except for the variable under consideration.

Table 14

	1	2	3	4	5	6
m	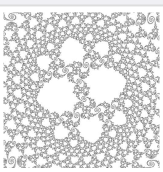 Figure 17	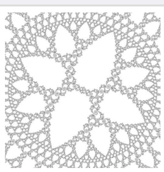 Figure 18	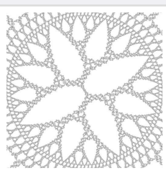 Figure 19	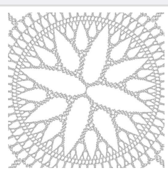 Figure 20	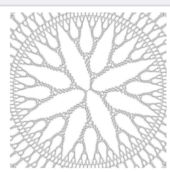 Figure 21	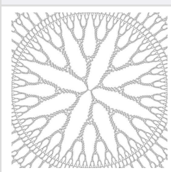 Figure 22

k/5	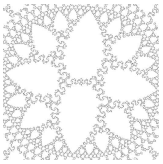 Figure 23	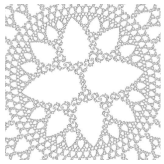 Figure 24	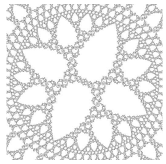 Figure 25	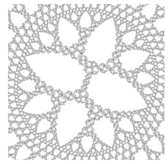 Figure 26	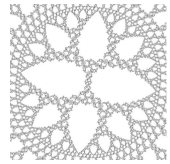 Figure 27	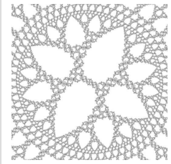 Figure 28

"Evolution of Trees" variations

Combining the previous two synthesized variations to simplify, and reduce the periods to make ray tracing feasible:

Table 15

P(n) (Period)	O(P) (Lower External Angle)	I(P) (Upper External Angle)
1	0	1
i	$0\ 1^{i-1}$	$1\ 0^{i-1}$
$((j+1)\times 2+k)\times i+1$	$(O(i)\ I(i))^j\ O(i)\ O(i)\ I(i)^k\ 1$	$(O(i)\ I(i))^j\ O(i)\ I(i)\ O(i)^k\ 0$
$P(n-1)+l\times i+1$	$O(n-1)\ O(i)\ I(i)^l\ 1$	$O(n-1)\ I(i)\ O(i)^l\ 0$
$2\times P(n-1)+2+(m+1)\times i$	$O(n-1)\ O(n-1)\ 0\ I(i)^{m+1}$	$I(n-1)\ I(n-1)\ 1\ O(i)^{m+1}$
$P(n-1)+2\times P(n-2)+2+(m+1)\times i$	$O(n-1)\ O(n-2)\ I(n-2)\ 11\ O(i)^{m+1}$	$O(n-1)\ I(n-2)\ O(n-2)\ 00\ I(i)^{m+1}$
$P(n-1)+2\times P(n-2)+m\times i$	$O(n-1)\ O(n-2)\ I(n-2)\ O(i)^m$	$I(n-1)\ O(n-2)\ O(n-2)\ I(i)^m$
$P(n-1)+2\times P(n-2)+m\times i$	$O(n-1)\ I(n-2)\ O(n-2)\ O(i)^m$	$I(n-1)\ O(n-2)\ I(n-2)\ I(i)^m$

Increasing i lengthens and straightens the filaments, by choosing an island further along the needle. Increasing j increases the spiral count, by choosing a bulb deeper in Seahorse Valley. Increasing k tightens the spirals, by choosing an embedded Julia set closer to the root of the hair. Increasing l makes the trees bigger and closer together. Increasing m makes the branches of the trees longer, by choosing nodes further from the centre. Repeating the final step an increasing number d times makes the overall structure more refined. Images drawn with $i = 5$, $j = 3$, $k = 3$, $l = 3$, $m = 3$, $d = 5$ except for the variable under consideration.

Table 16

	1	2	3	4	5	6

i-2	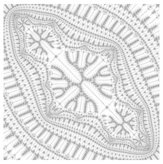 Figure 29	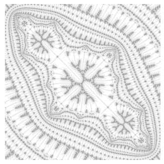 Figure 30	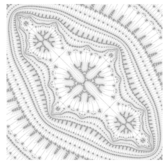 Figure 31	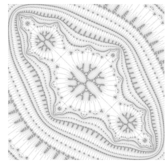 Figure 32	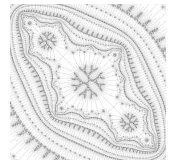 Figure 33	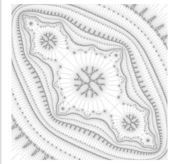 Figure 34
j	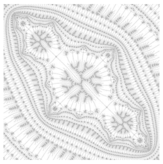 Figure 35	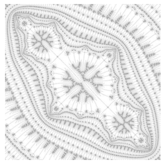 Figure 36	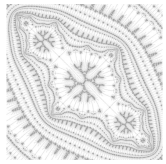 Figure 37	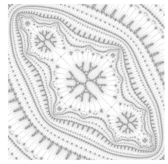 Figure 38	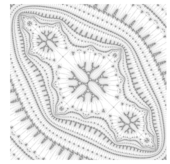 Figure 39	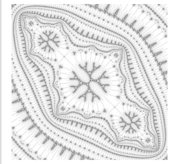 Figure 40
k	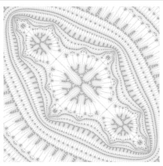 Figure 41	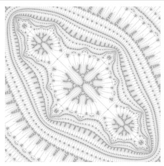 Figure 42	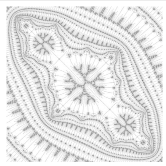 Figure 43	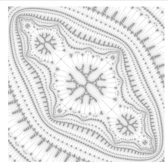 Figure 44	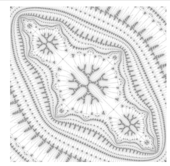 Figure 45	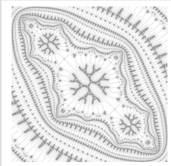 Figure 46
l	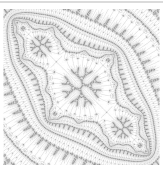 Figure 47	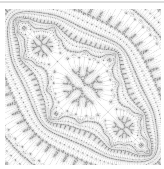 Figure 48	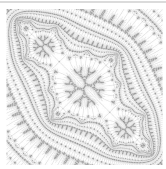 Figure 49	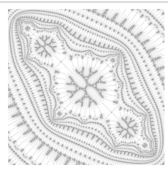 Figure 50	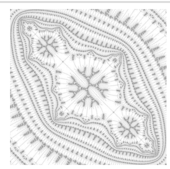 Figure 51	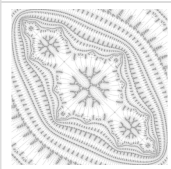 Figure 52
m	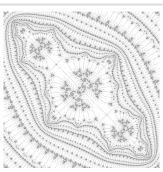 Figure 53	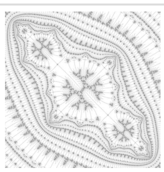 Figure 54	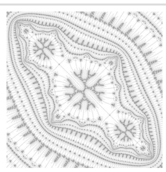 Figure 55	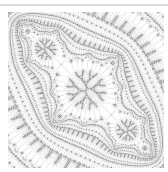 Figure 56	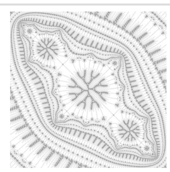 Figure 57	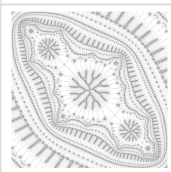 Figure 58
d+1	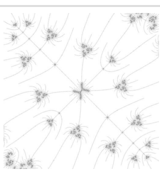 Figure 59	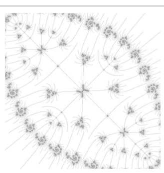 Figure 60	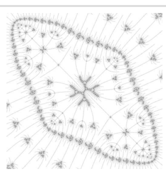 Figure 61	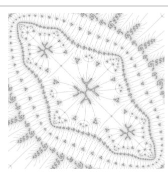 Figure 62	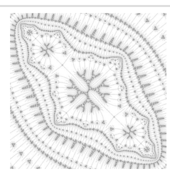 Figure 63	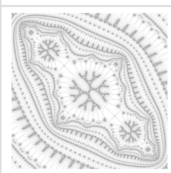 Figure 64

Conclusions

Patterns in deep Mandelbrot set zoom artworks by several artists were analyzed and compared. Different variations on these patterns were synthesized. Assisted zooming in existing fractal software (principally period detection, root finding, and target zoom level estimation) supports this line of artistic enquiry. Full analysis and synthesis automation via external ray tracing currently remains out of reach for high period examples due to computational constraints.

References

1. Devaney, Robert L. 1999. "The Mandelbrot Set, the Farey Tree, and the Fibonacci Sequence." *The American Mathematical Monthly* 106 (4): 289–302. https://doi.org/10.1080/00029890.1999.12005046. ↩

2.
"Chaotic series of fractal articles"

Ingvar Kullberg

<http://klippan.seths.se/fractals/articles/>

↩

3. Douady, A. 1986. "ALGORITHMS FOR COMPUTING ANGLES IN THE MANDELBROT SET." In *Chaotic Dynamics and Fractals*, 155–68. Elsevier. https://doi.org/10.1016/b978-0-12-079060-9.50014-x. ↩

4. Schleicher, Dierk. 1997. "Rational Parameter Rays of the Mandelbrot Set." *arXiv*. https://doi.org/10.48550/ARXIV.MATH/9711213. ↩

5.
"Symbolic dynamics of quadratic polynomials"

Henk Bruin and Dierk Schleicher

Reports Institut Mittag-Leffler Preprint series: Probability and Conformal Mappings - 2001/2002, No. 07, Institut Mittag-Leffler, Stockholm, Sweden, 2001-2002 ISSN: 1103-467X ISRN: IML-R

<https://web.archive.org/web/20040822172738/http://www.ml.kva.se/preprints/archive/2001-2002/2001-2002-07.pdf> ↩

6.
"An algorithm to draw external rays of the Mandelbrot set"

Tomoki Kawahira

<https://www1.econ.hit-u.ac.jp/kawahira/programs/mandel-exray.pdf>

↩

7.

“Leavittation”

Images in GIF format exported from FractInt, which contain embedded metadata including the coordinates and palette.

<http://web.archive.org/web/20010112000300/http://www.sky-dyes.com/leavitt1.html>;↩

8.

“My Favorite Fractals”

Images in GIF format exported from FractInt, which contain embedded metadata including the coordinates and palette.

<http://web.archive.org/web/20010127022300/http://sky-dyes.com:80/favefractals.html>; ↩

9.

MDZ Gallery

<https://web.archive.org/web/20130126074606/http://www.jwm-art.net:80/mdz/gallery/>

↩

10.

MDZ Gallery (mirror)

<https://mathr.co.uk/mdz/gallery>

↩

11.

FractalMonster’s gallery on Deviant Art

<https://www.deviantart.com/fractalmonster/gallery>

↩

12.

DinkydauSet’s Mandebrot set gallery on Deviant Art

<https://www.deviantart.com/dinkydauset/gallery/35248203/mandelbrot-set>

↩

13.

Microfractal's Mandelbrot Deep Julia Morphing Images gallery on Deviant Art

<https://www.deviantart.com/microfractal/gallery/77607498/mandelbrot-deep-julia-morphing-images>

↩

14.
Olbaid-ST's Deep Mandelbrot Set gallery on Deviant Art

<https://www.deviantart.com/olbaid-st/gallery/62665794/deep-mandelbrot-set>

↩

15.
"Polefcra"

<http://web.archive.org/web/20010303051520/http://sky-dyes.com/polefcra.html>

↩

16.
"Old Wood Dish"

<https://mathr.co.uk/mdz/gallery/#oldwooddish>

↩

17.
"Evolution Of Trees"

<https://www.deviantart.com/dinkydauset/art/Evolution-of-trees-402876071>

↩

18.
"Mandelbrot Deep Julia Morphing 1"

<https://www.deviantart.com/microfractal/art/Mandelbrot-Deep-Julia-Morphing-1-873185063>; ↩